



CANADIAN SEISMIC DESIGN PROVISIONS FOR SINGLE-STOREY BUILDINGS WITH FLEXIBLE METAL ROOF DECK DIAPHRAGMS

R. Tremblay⁽¹⁾, C.A. Rogers⁽²⁾

⁽¹⁾ Professor, Dept. of Civil, Geological, and Mining Eng., Polytechnique Montréal, Canada, robert.tremblay@polymtl.ca

⁽²⁾ Professor, Dept. of Civil Eng. and Applied Mechanics, McGill University, Montreal, Canada, colin.rogers@mcgill.ca

Abstract

The article presents the seismic design provisions that have been introduced in the 2015 edition of the National Building Code of Canada for single-storey steel buildings with flexible metal roof deck diaphragms. A new period empirical formula that accounts for the structure height and the length of the roof diaphragm between vertical bracing is now specified for these structures. Dynamic amplification of diaphragm shears and bending moments due to higher mode response must now be considered in the design of the roof diaphragm, in addition to capacity design provisions that existed in previous code editions. The code also requires that the deformation demands on the vertical bracing elements be verified in design to avoid excessive deformations causing rupture in the vertical systems. Simple methods are proposed in the article to predict diaphragm internal forces and lateral deformations of the vertical bracing for design purposes.

The new code provisions and proposed assessment methods are applied for two simple prototype buildings with lateral resistance provided by tension-compression (T/C) concentrically braced frames (CBFs), tension-only (T/O) CBFs, and eccentrically braced frames. The latter two systems are considered promising alternatives to the common TC CBFs, especially for reducing the forces that must be considered for the design of the roof diaphragm. A building structure with an intermediate braced line at its mid-length is also considered to examine the verify if design provisions developed for structures with vertical bracing located in the end walls can lead to satisfactory seismic response for structures with interior bracing. Nonlinear response history analysis was performed to investigate the responses of the structures and validate the new design provisions and assessment methods.

The study confirmed the possibility of reducing significantly design diaphragm forces when using the T/O CBF or EBF system. Results from the nonlinear dynamic analyses showed that the assessment methods for diaphragm forces and braced frame deformations give satisfactory results for buildings with T/C CBFs. However, the methods were found to significantly underestimate the seismic demand on diaphragm and braced frames when T/O CBFs or EBFs are used. Structures with both systems experienced excessive storey drifts and additional design guidance is needed to ensure proper seismic response for structures built with these systems. The nonlinear analysis results also showed that the building constructed with an interior bracing line responded predominantly as a structure with end bracing only, with inelastic deformations concentrating in the interior braced frames. Further studies are needed to understand better the nonlinear response of these structures and propose provisions that can be implemented to ensure more uniform inelastic deformation demands on the vertical bracing elements.

Keywords: Steel braced frames; Steel roof deck diaphragm; Diaphragm flexibility; Design period; Dynamic amplification



1. Introduction

In Canada, steel structures are commonly used for single-storey buildings that are employed for industrial, recreational, and commercial applications. In these structures, the roof structure typically includes corrugated steel roof deck panels supported on a roof frame consisting of open-web steel joists and I-shaped steel girders (Fig. 1a). I-shaped or tubular steel members are used for the columns. The roof deck panels are connected to each other and to the supporting structure to form an in-plane diaphragm capable of collecting and transferring to the vertical bracing elements lateral loads due to winds and earthquakes. As illustrated in Fig. 1a, vertical bracing elements are generally placed along the building perimeter to minimize obstruction in the structure. Lateral loads induce in-plane shear forces and bending moments in the roof diaphragm, causing horizontal in-plane deformations of the diaphragm, Δ_D , that add to the deflection of the vertical bracing, Δ_B (Fig. 1b).

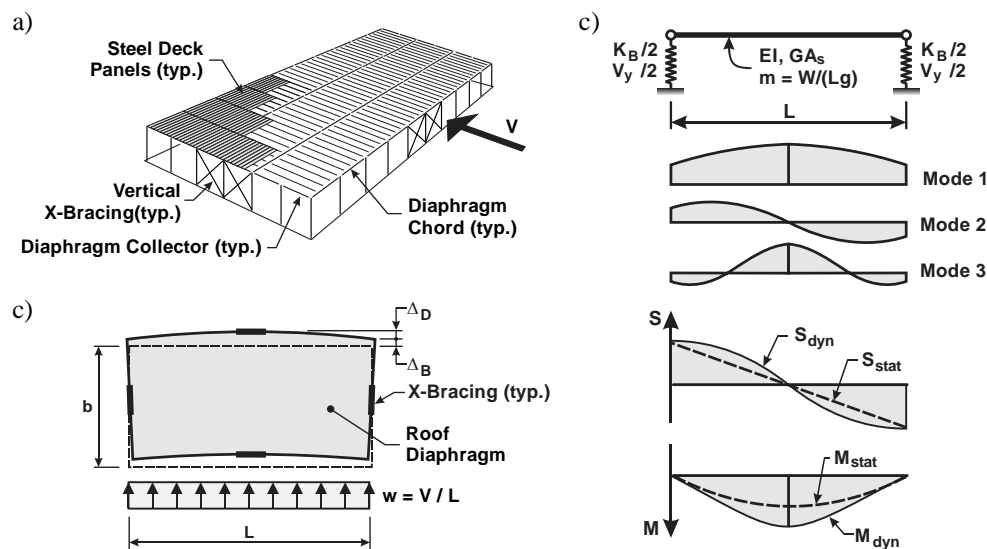


Fig. 1 - Single-storey steel building with flexible roof deck diaphragm and perimeter vertical bracing:
 a) Structure overview; b) Lateral deformation of the roof diaphragm (Δ_D) and vertical bracing (Δ_B);
 c) Structure vibration modes and dynamic amplification of diaphragm shears and moments

For these buildings, the flexibility of the roof deck diaphragm has significant effects on the structure response to earthquake ground motions. The structure fundamental period is lengthened compared to the structures with rigid roof diaphragms, which generally results in reduced seismic inertia lateral loads and increased lateral displacements [1-5]. As shown in for the case of a structure with lateral bracing along the end walls, the structure lateral response is also contributed by several modes of vibration resulting from in-plane roof diaphragm deformations (Fig. 1c). Force demand from first mode response is mostly controlled by the yield strength of the vertical bracing elements, as is the case for structures with rigid diaphragms; however, higher vibration modes can induce significant additional in-plane shears and bending moments in roof diaphragms [6-9], as schematically illustrated in Fig. 1c. If the diaphragm is designed to resist these dynamically magnified forces, inelastic deformations concentrate in the vertical bracing elements and the imposed ductility may exceed the value of the force modification factor used in design [10] as yielding is limited to only one of the two components acting in series in the seismic force resisting system (SFRS). The design must then be adjusted so that the anticipated inelastic demand remains below the plastic deformation capacity of the vertical bracing.

Specific provisions have been introduced in the 2015 edition of the National Building Code (NBC) of Canada [11] to address these effects from roof diaphragm flexibility in seismic design. Those include a new



expression is specified for the building fundamental period to obtain more realistic, yet conservative estimates of the elastic force demand for design. The period in that formula depends on the building height and diaphragm length. The NBC requires that floor and roof diaphragms in buildings remain essentially elastic to maintain the integrity of the SFRS during an earthquake. This general rule also applies to steel roof deck diaphragms of single-storey buildings. This behaviour is also justified because the diaphragm provides lateral bracing to roof joists and beams and this function must be preserved to prevent collapse of the gravity framing. It is also deemed that damage to roof diaphragms would be difficult and costly to inspect and repair after an earthquake and limiting inelastic demand in vertical bracing represents a good seismic design practice. To achieve this behaviour, capacity design principles is enforced, requiring that design diaphragm forces be obtained from the probable resistance of the SFRS vertical elements. NBC requires that dynamic amplification of shears and bending moments be considered in diaphragm force calculations. NBC also requires that inelastic deformations in the vertical bracing be within acceptable limits for the bracing system selected, which requires an evaluation of the inelastic deformation demand on these elements. When deformations are found to be excessive, NBC proposes a simple equation to adjust the force modification factor to limit the ductility to the system capacity. The method has been developed and validated mainly for simple rectangular buildings constructed with concentrically steel braced frames (CBFs) on the perimeter walls, as shown in Fig. 1. For this common configuration, it was found that braced frames can generally accommodate the deformation demand resulting from code specified force modification factors, without adjustments [9].

The NBC seismic provisions for single-storey steel buildings are briefly reviewed in the first section of the article. Application of the provisions is then illustrated for two simple rectangular buildings having different floor areas and length-to-width aspect ratios. CBFs with bracing members acting in compression and tension are examined, together with two possible bracing alternatives: CBFs with tension-only bracing members and eccentrically braced frames. These two options are expected to result in lower diaphragm design forces because of their inherent greater flexibility and longer periods, as well as their inherent lower lateral overstrength. However, this may come at the expense of larger lateral displacements that can lead to excessive inelastic deformation demands. Finally, a building with an intermediate bracing line at the building mid-length is also studied to verify the approach commonly adopted in practice according to which the SFRS can be designed as if the building consisted of individual rectangular structures with perimeter bracing. The prototype structures were assumed to be built in the region of Vancouver, British Columbia, a region exposed to three different sources of earthquakes, including interface subduction earthquakes capable of imposing large displacement demands on structures. Nonlinear response history analysis of the structures was performed to assess their response and validate the design methodology.

2. NBC Seismic Provisions for Single-Storey Buildings with Flexible Roof Diaphragms

In the 2015 NBC, the minimum design seismic load, V , is given by:

$$V = \frac{S(T_a) M_V I_E W}{R_d R_o} \quad (1)$$

where S is the design spectrum, T_a is the building fundamental period of vibration for design, M_V accounts for higher mode effects on base shear for multi-storey buildings, I_E is the importance factor, W is the seismic weight, and R_d and R_o are respectively the ductility- and overstrength-related force modification factors. The design spectrum is obtained from the products of site coefficients $F(T)$ and uniform hazard spectral (UHS) accelerations $S_a(T)$ specified at periods $T = 0.2, 0.5, 1.0, 2.0, 5.0,$ and 10 s. Site coefficient values depend on the site class and the reference peak ground acceleration at the site, PGA_{ref} . The S_a values are specified for a probability of exceedance of 2% in 50 years. The design spectra for the location and site condition (site class E) considered in this study is plotted in Fig. 2a for illustration. Only the short period range is shown. In Eq. (1), M_V takes a value of 1.0 for single-storey buildings. The importance factor I_E in Eq. (1) depends on the risk category of the building: from 1.0 for buildings of the normal risk category, as those studied herein, to



1.5 for post-disaster buildings. The seismic weight W is equal to the dead load plus 25% of the design roof snow load. The factor R_d ranges from 5.0 for the most ductile systems to 1.0 for brittle ones [2]. The R_o factor reflects the dependable lateral overstrength of the SFRS. It varies between 1.0 and 1.5 depending on the SFRS. For steel CBFs of the moderately ductile (Type MD) category, values of 3.0 and 1.3 are respectively specified for R_d and R_o in the NBC. These factors take values of 4.0 and 1.5 for ductile (Type D) eccentrically braced steel frames. For short period structures with minimum ductility ($R_d \geq 1.5$), the force V from Eq. (1) need not exceed 2/3 the value computed at a period of 0.2 s, but not less than V at 0.5 s. The resulting design base shear (V/W) for the two SFRSs are plotted in Fig. 2a for the site under consideration.

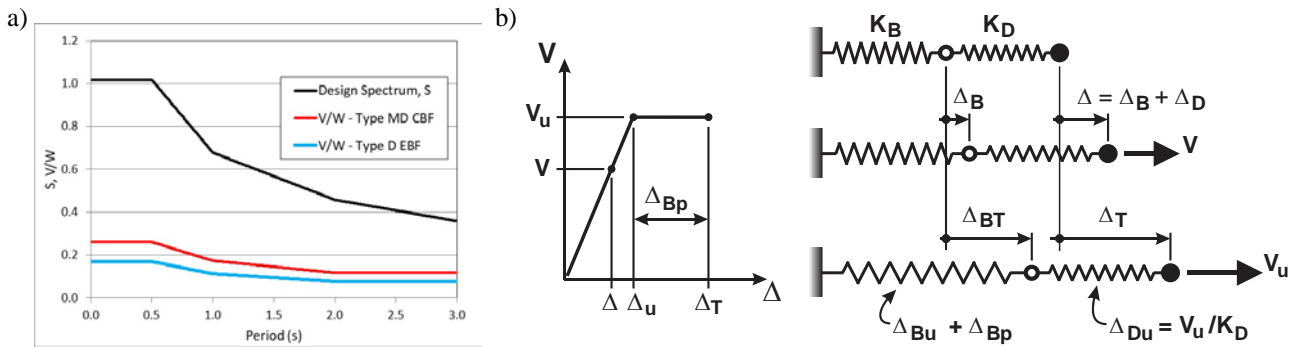


Fig. 2 – a) Design spectrum and design seismic loads for site class E in Vancouver, BC; b) Displacement demands on the vertical bracing elements of single-storey buildings with flexible roof diaphragms

The period of vibration T_a can be taken as the fundamental period of the structure from dynamic analysis, T_1 . When determining the seismic load V for strength requirements, however, T_a cannot exceed an upper limit corresponding to 1.5 times the period obtained from the new empirical equation reflecting period lengthening due to diaphragm flexibility:

$$T_a = 0.035h_n + 0.004L \quad (2)$$

where L is the diaphragm span between adjoining vertical braced frames (in meters). This upper limit on T_a does not apply for drift calculations and the seismic load V_Δ obtained from Eq. (1) with the period $T_a = T_1$ is permitted to be used to calculate drifts. For regular buildings with vertical bracing at the diaphragm ends shown in Fig. 1, the period T_1 can be estimated from [6, 12]:

$$T_1 \approx 2\pi \sqrt{\frac{W}{g} \frac{(\Delta_B + 0.76\Delta_D)}{V}} = T_B \sqrt{1 + 0.76 \frac{\Delta_D}{\Delta_B}}, \text{ where: } T_B = 2\pi \sqrt{\frac{W}{g K_B}} \quad (3)$$

where Δ_B and Δ_D are respectively the lateral deformation of the vertical bracing and the relative in-plane deformation of the roof diaphragm under an arbitrarily uniformly distributed static load V/L (see Fig. 1b), g is the acceleration due to gravity, T_B is the fundamental period of the structure assuming rigid diaphragm conditions, and K_B is the total lateral stiffness of the vertical bracing elements ($\Delta_B = V/K_B$). To obtain a first design trial, seismic loads are typically determined using the period T_a from Eq. 2. In subsequent iterations, the period T_a and seismic loads are progressively adjusted based on stiffness properties obtained from the previous iteration.

In design, vertical bracing elements are first designed to resist forces from the seismic load plus concomitant gravity loads. For single-storey buildings, the latter includes the dead load plus 25% of the design roof snow load ($D + 0.25 S$). The probable lateral resistance of the vertical bracing, V_u , is then evaluated using probable yield strength and accounting for strain hardening effects. According to capacity design, the design shear at the diaphragm ends is determined from the lateral force V_u . Furthermore, the NBC now requires that diaphragm shears and moments along the diaphragm span be evaluated with consideration



of dynamic amplification from higher mode response. This new requirement only applies when $R_d > 1.5$ and $\Delta_D/\Delta_B > 0.5$, i.e. when minimum inelastic response is anticipated, and roof diaphragm flexibility is relatively important. However, the NBC does not prescribe any specific method to obtain these dynamically magnified design forces. In this study, it is proposed to use a modified response spectrum analysis (RSA) performed with the simple beam model with flexible supports shown in Fig. 1. Two analyses are conducted using the NBC spectrum S as input: the first analysis considering only the first vibrational mode (mode 1), and the second analysis considering all contributing modes. For symmetrical buildings as discussed here, only odd numbered modes need to be included as even numbered modes are not excited when the same seismic input is applied at both supports. Shears and moments from higher modes, i.e. the 3rd, 5th and subsequent modes, are obtained by subtracting the results of the first analysis from those of the second analysis. Diaphragm in-plane shear $V(x)$ is then obtained by combining the contribution from the first mode, $V^1(x)$, to that from the higher modes, $V^{3+}(x)$, using:

$$V(x) = \alpha V^1(x) + V^{3+}(x) \quad , \text{where: } \alpha = \frac{V_{u,\text{Wall}} - V^{3+}(x=0)}{V^1(x=0)} \quad (4)$$

An absolute sum is adopted assuming that both contributions can reach their peaks simultaneously. The first mode contribution is multiplied by a scaling factor α determined such that the total shear at the diaphragm end, $\alpha V^1 + V^{3+}$, is equal to $V_{u,\text{Wall}}$, where $V_{u,\text{Wall}}$ is the total probable resistance of the bracing bays along the end wall. Contributions αV^1 and V^{3+} and the combined shear used for design are illustrated in Fig. 3a for the diaphragm of the C-T/C Building B studied later. For this structure, $V_{u,\text{Wall}}$ is equal to 2590 kN and V^1 and V^{3+} from RSA were respectively equal to 4471 kN and 307 kN, which resulted in $\alpha = 0.548$. As shown, the design shear at $0.25 L$ is approximately 50% higher than the value obtained with the linear variation from static analysis. Design shears for all buildings examined in this study are plotted in Fig. 3b. For the same building (A or B), the large differences are due to the different $V_{u,\text{Wall}}$ values obtained for the different vertical bracing systems considered. The method is also used for moments in the diaphragm, with the first mode moments being multiplied by the α factor determined with end shears.

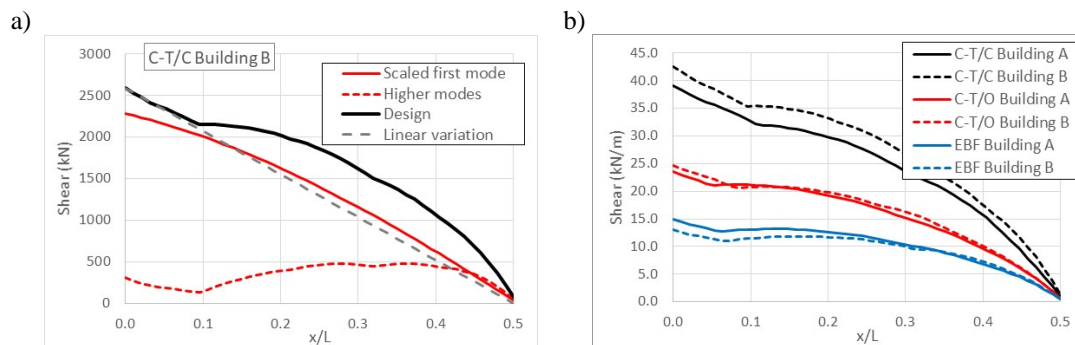


Fig. 3 –Diaphragm shears including dynamic amplification from higher mode response: a) Contributions from first and higher modes plus combined effects for the C-T/C Building B; b) Design shears for all buildings of this study.

The last provision introduced in NBC 2015 for single-storey buildings with flexible diaphragms is the verification of the inelastic deformation demand on the vertical bracing elements. This requirement also only applies to structures designed with $R_d > 1.5$ and when $\Delta_D/\Delta_B > 0.5$. Two options are offered in NBC: 1) to evaluate the anticipated deformation demand and verify that it can be accommodated by the selected bracing system, or 2) to increase the design seismic loads so that the ductility demand on the vertical bracing elements remains same as if the building had a rigid diaphragm. It is expected that the first option will be the preferred one in practice because it will likely result in more cost-effective designs compared to the second option which will require stronger vertical bracing elements that will, in turn, impose higher force demands for the design of the roof diaphragm. The first option was therefore adopted herein. In the NBC, the



maximum anticipated structure lateral displacement including inelastic response, Δ_T , is assumed to be equal to the displacement under the elastic (unreduced) forces, i.e. $\Delta_T = (\Delta_B + \Delta_D) \times R_d R_o$. As illustrated in Fig. 2b, the total deformation in the vertical bracing elements when this displacement is reached, Δ_{BT} , can be estimated as $\Delta_T - \Delta_{Du}$, where Δ_{Du} is the diaphragm deflection under the lateral load V_u . The deformation capacity of the vertical bracing elements can then be verified using the total deformation Δ_{BT} or the plastic deformation $\Delta_{BP} = \Delta_{BT} - \Delta_{Bu}$, where Δ_{Bu} is the vertical bracing deformation under the lateral load V_u , depending on the deformation criteria that is employed for the assessment. In these calculations, Δ_T can be calculated with Δ_B and Δ_D obtained from static analysis of the SFRS under the seismic load V_Δ computed with the period T_1 . Alternatively, Δ_T can be obtained directly from the second response spectrum analysis considering all contributing modes that is performed for evaluating diaphragm shears and moments.

Roof diaphragm flexibility increases lateral displacements and code limits on storey drifts may control the design of the vertical bracing and/or roof diaphragm. In the NBC, the storey drift limit varies from 1% h_s for post-disaster buildings to 2.5% h_s for buildings of the normal risk category, where h_s is the storey height (or building height for single-storey buildings). The computed displacement Δ_T must therefore be verified against the applicable limit.

In Canada, steel SFRSs with R_d equal to or greater than 1.5 must be designed and detailed in accordance with the special seismic provisions included in the CSA S16-14 standard [13]. Those provisions include severe limits on cross-section slenderness for the SFRS yielding members, such as bracing members in CBFs and link beams in EBFs. Limits are also specified on CBF brace overall slenderness as well as on plastic rotation of EBF link beams. Strict capacity design provisions must also be followed the non-yielding SFRS elements. CSA S16 and NBC 2015 also include

3. Building Examples

3.1 Building design

Application of the NBC new provisions is illustrated for the two steel buildings shown in Fig. 4. Building A represents a sport facility with a total height of 6.6 m, a clear span of 31 m and an aspect ratio of 2.4. Building B is taller (8.2 m vs 6.6 m) and has a larger footprint, which is typical for industrial or warehouse usages. Building B has a length-to-width ratio of 1.5. The roof framing consists of 12.4 m or 15.2 m long open web steel joists supported on steel I-beams. The roof dead and snow loads and weight of the exterior wall cladding are given in the figure.

The structures are examined in the direction perpendicular to the long walls, for which diaphragm flexibility effects are more pronounced. As indicated, the structures are located near Vancouver, BC, on a soft soil (class E) site. The design spectrum for this site is shown in Fig. 3a. As shown in Fig. 4 CBFs with an X-bracing configuration are used for both structures. Single-bay bracing was selected for Building A whereas two-bay bracing was chosen for Building B to avoid large brace forces and column base reactions that require costly construction details. Both tension-compression (T/C) and tension-only (T/O) bracing were considered for the two buildings, as this difference can significantly affect the structure cost and seismic response. T/C and T/O CBFs are thereafter referred to as C-T/C and C-T/O. These braced frames were designed as Type MD CBFs with force modification factors $R_d = 3.0$ and $R_o = 1.3$. For both building sizes, the ductile (Type D) eccentrically braced frame (EBF) is also considered because it is expected to result in lower seismic loads due to its higher values of the R_d (4.0) and R_o (1.5) factors and its inherent greater flexibility and longer periods. Short links yielding in shear were however chosen to control storey drifts.

A third building geometry, not shown in Fig. 4, was created by connecting end-to-end two Buildings B to form a 60.8 m wide x 182.4 m long structure with one interior bracing line at the building mid-length. This building is referred to as “2xB Building”. For this structure, only the C-T/C system was considered. Design and behaviour of this structure are discussed in Section 3.3.



The vertical bracing elements were designed in accordance with the CSA S16-14 standard. Square hollow structural shapes (SHS) conforming to ASTM A1085 with a specified yield strength of 345 MPa were used for the columns and bracing members. Brace global slenderness was determined with an effective brace length equal to 0.45 times the working point dimension to account for the support at the brace interesting point and the size of the end connections. Beams were assumed to be I-shapes conforming to ASTM A992 ($F_y = 345$ MPa). The roof diaphragms were made of 914 mm wide x 38 mm deep wide rib steel deck panels. The panels were made from ASTM A653 steel with $F_y = 410$ MPa and $F_u = 480$ MPa. The design was performed using the AISI S310-16 standard [14]. In Fig. 4, roof diaphragms were divided into four zones in which diaphragm design was adjusted so that the shear resistance could envelop the design shear forces presented in Fig. 3b. For panels made of 1.21 mm and 1.52 mm thick steel, support connections consist of 19 mm diameter arc spot welds with $F_u = 410$ MPa whereas #14 self-drilling screws were chosen used for the side-lap connections. Deck panels with 0.91 mm thick steel were connected to the structure with Hilti X-HSN24 powder-actuated fasteners and assembled together with #12 screw side-lap connections.

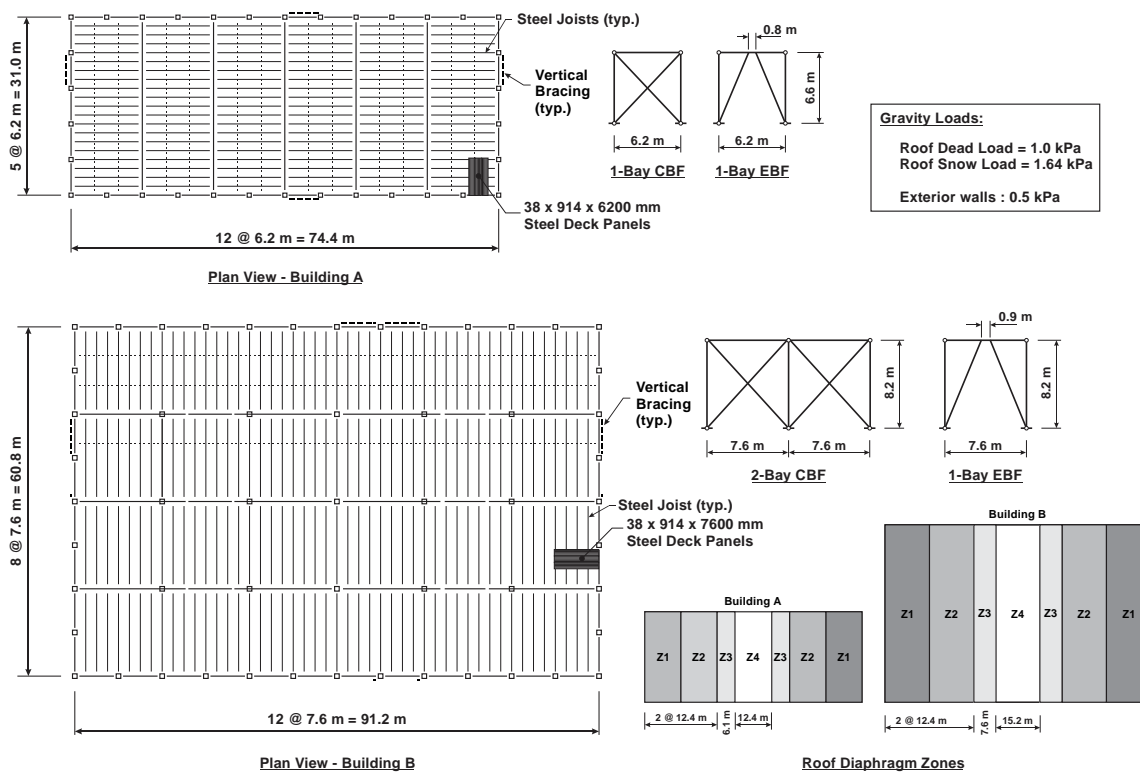


Fig. 4 – Structures studied

The properties of the structures are summarized in Table 1 and details of the diaphragm design for each zone are given in Table 2. The periods obtained from Eq. (2) are equal to 0.53 and 0.65 s for Buildings A and B, respectively, giving upper limit on periods of 0.79 and 0.98 s for strength requirements. For the calculation of V in Eq. (1), factors I_E and M_V were set equal to 1.0. Accidental torsional effects were omitted for simplicity; braced frames along each end wall were therefore designed for 50% of the total seismic load. Braces in the C-T/C frames were designed for compressive resistance, which required larger cross-sections than their C-T/O counterparts. For the C-T/O frames, only one of the two braces per frame was considered in the stiffness K_B , which resulted in longer periods T_B in Table 1 (T_B is determined assuming rigid diaphragm – see Eq. 2). As expected, the EBF systems are also more flexible than the corresponding C-T/C frames, as also evidenced by their longer periods T_B . The computed periods T_1 are longer than T_a from Eq. 2, except for Building B with C-T/C which has T_1 (0.61 s) slightly lower than the empirical value of 0.65 s. For the two C-T/C buildings and the C-T/O Building B, the design period was controlled by T_1 . For the other buildings, the design period for strength requirements was limited by the upper limit on period specified in the NBC.



Table 1: Design values and SFRS properties

Building	A			B			2xB
Dimensions	31.0 m x 74.4 m x 6.6 m			60.8 m x 91.2 m x 8.2 m			-
W (kN)	3600			8442			16884
SFRS type	C-T/C	C-T/O	EBF	C-T/C	C-T/O	EBF	C-T/C
n frames/wall	1	1	1	2	2	1	2
T_B (s)	0.38	0.60	0.63	0.43	0.76	0.78	0.46
T_1 (s)	0.58	0.87	0.81	0.61	0.90	0.98	0.62
T_3 (s)	0.18	0.26	0.23	0.22	0.24	0.23	0.38
T_a (s)	0.58	0.79 ¹	0.79 ¹	0.61	0.90	0.98 ¹	0.61 ²
V / building (kN)	896	758	492	2040	1616	982	4080 ²
V/W	0.249	0.211	0.137	0.242	0.191	0.116	0.242 ²
Brace SHS	102x7.9	76x7.9	203x6.4	127x6.4	76x7.9	203x13	152x9.5 ³
Brace KL/r	108	146	-	103	185	-	87 ³
Link beam	-	-	W310x39	-	-	W410x60	-
Columns (SHS)	203x7.9	203x6.4	152x6.4	254x7.9	254x6.4	178x6.4	305x9.5 ³
V_u / building (kN)	2426	1532	922	5180	2872	1582	4920 ³
V_u / V	2.71	2.02	1.87	2.54	1.78	1.61	2.41 ³
$S_{f,max}$ (kN/m)	39.1	24.7	14.9	42.8	23.6	13.0	42.8 ⁴
I_D (10^{12} mm ⁴)	3.91	2.75	2.72	25.0	15.9	11.9	25.0
V_Δ / building (kN)	896	708	484	2040	1464	982	4080
Δ_B (mm)	9.06	13.8	13.4	11.2	24.8	17.6	10.4/13.7 ⁵
Δ_D (mm)	16.2	30.8	12.6	17.4	16.7	15.2	16.8
Δ_D / Δ_B	1.79	2.23	1.99	1.55	0.67	0.86	1.40 ⁶
Δ_T (mm)	98.7	174	156	112	162	197	113
Δ_T (% h_n)	1.50	2.63	2.36	1.37	1.98	2.40	1.38
Δ_{BT} (mm)	54.8	112	133	67.8	130	173	72.5
$\Delta_{T,RSA}$ (mm)	105	182	163	123	180	207	123
$\Delta_{BT,RSA}$ (mm)	56.7	124	137	71.7	146	180	78.1/71.9 ⁵

¹Governed by the code upper limit on T_a

²Design lateral load for the interior bracing bays taken as 2.0 times the C-T/C value for Building B

³Properties for the interior bracing bays; exterior bracing bays are same as C-T/C of Building B

⁴Diaphragm shears taken equal to those considered for the C-T/C Building B

⁵Values at the exterior and interior braced lines, respectively

⁶Average ratio for the exterior and interior braced lines

Table 2: Diaphragm design and shear stiffness G' in zones Z1 to Z4 (see Fig. 4)

Building	A			B		
Zone	C-T/C	C-T/O	EBF	C-T/C	C-T/O	EBF
Z1	1.21-7/12 32.1 ¹	1.21-4/9 10.7	0.91-7/9 20.7	1.52-7/12 40.4	1.21-7/6 25.9	0.91-7/8 20.1
Z2	1.21-7/8 29.2	1.21-4/5 9.99	0.91-7/7 19.6	1.21-7/13 32.2	1.21-7/4 23.0	0.91-7/10 19.5
Z3	1.21-4/5 9.99	0.91-7/8 20.2	0.91-7/4 17.4	1.21-4/10 12.1	0.91-7/9 20.7	0.91-4/9 6.76
Z4	0.91-7/6 12.5	0.91-4/5 5.62	0.91-4/2 5.15	0.91-4/9- 6.78	0.91-4/5 6.34	0.91-4/4 6.17

¹ "1.21-7/12 32.1" = 1.21 mm thick steel; 7 support connections over the 914 mm panel width; 12 side-lap connections per joist span; and $G' = 32.1$ kN/mm

For the C-T/C frames, the difference between probable brace tension and compressive resistances resulted in large probable lateral strength V_u and system overstrength V_u/V of 2.54 in Building A and 2.71 for Building B, close to the R_d value of 3.0 used in design. This resulted in high shear force demand $S_{f,max}$ at the end of the roof diaphragm in Table 1 and along the diaphragm span as shown in Fig. 3b. Braces in C-T/O frames are much slender and their compressive resistances have limited contribution to the probable strength V_u and system overstrength V_u/V . EBFs possess even lower system overstrength and, thereby, required much



lighter diaphragm designs compared to the two CBF systems. In Table 2, deck panels with 0.91 mm thick steel can be used over the entire roof area of EBF Buildings A and B. For the CBF systems, thicker deck material was needed in 2 or 3 zones of the roof area. For the C-T/O and EBF systems, the more flexible diaphragm designed resulted in longer frame periods, reduced design seismic loads and, thereby, lower resistances V_u and design shears S_f for the roof diaphragms.

The seismic load V_Δ determined with the actual period T_1 and the resulting deflections Δ_B , Δ_D , and Δ_T are given in Table 1. As shown, for all structures, the Δ_D/Δ_B exceeds the 0.5 threshold value beyond which diaphragm flexibility effects must be accounted for in design. The storey drift Δ_T satisfies the NBC limit of 2.5% h_n for all structures but the C-T/O Building A for which the limit is slightly exceeded (2.63% h_n). The predicted deformations Δ_{BT} are also given in the Table. For the two CBF-T/C structures, these deformations impose a brace ductility of 1.8 based on probable yield strength. The ductility demand on the braces of the C-T/O frames are respectively equal to 3.4 and 3.8 for Buildings A and B. These ductility levels can be accommodated by bracing members detailed in accordance with the CSA S16 provisions. Plastic rotations of 0.13 and 0.15 radians are evaluated in the EBF links of Buildings A and B based on the computed Δ_{BT} values for these two frames. This significantly exceeds the CSA S16 limit of 0.08 radians for short links yielding in shear, and the frames should have been redesigned to meet this limit. This redesign was not performed herein as the main objective was to validate the methods used to predict the demand. For all buildings, storey drifts Δ_T and Δ_{BT} were also determined from RSA and the $\Delta_{T,RSA}$ and $\Delta_{BT,RSA}$ values are reported in Table 1. For all structures, these RSA values are higher than those determined with V_Δ by a margin varying from 3 to 12%

3.2 Results of Response History Analyses

Nonlinear response history analysis (NLRHA) was performed for each structure using an ensemble of 15 ground motion records selected and scaled as described in [15]. The ensemble included 3 suites of 5 records, one suite for each of the three earthquake sources contributing to the hazard for the site, i.e. crustal earthquakes, deep in-slab subduction earthquakes, and interface subduction earthquakes. The analyses were performed using the OpenSees platform with force-based beam-column elements reproducing brace inelastic buckling and tension yielding for the CBF structures [16] and zero-length nonlinear elements simulating shear yielding of the EBF link beams [17]. Other beams and columns in the frames were modelled with elastic beam elements. Elastic beam elements deforming in flexural and shear were used for the roof diaphragms. Geometric non-linearities were considered in the analysis and damping corresponding to 3% of critical in first mode was specified. Values of peak response parameters of interest are given in Table 3. The values reported correspond to the mean values of the larger 5 results out of the 15 results from the 15 ground motion records.

Table 3: Peak storey shears and storey drifts from NLRHA

Buildin	A			B			2xB
	g						
SFRS type	C-T/C	C-T/O	EBF	C-T/C	C-T/O	EBF	C-T/C
V_{max}/V_u	0.97	1.02	1.14	0.96	0.98	1.22	0.96/1.08 ²
Δ_T (mm)	110 (1.05) ¹	243(1.34)	215 (1.32)	137 (1.11)	291(1.62)	272(1.31)	118 (0.96)
Δ_{BT} (mm)	67.2 (1.19)	179 (1.44)	186 (1.36)	90.0 (1.26)	260 (1.78)	243 (1.78)	57/112 ³

¹ Values in brackets are ratios with respect to the corresponding RSA values in Table 1.

² Values at the exterior and interior braced lines; ratios wrt Table 1 values for Δ_{BT} are respectively 0.73 and 1.56

As shown, peak lateral forces reached the predicted probable resistances V_u for all CBF structures. For the EBF system, the NLRHA V_u values exceeded the predicted values, likely because of the excessive strain hardening response predicted by the numerical model at the large link shear deformations sustained by the EBFs. For all structures, peak storey drifts Δ_T and Δ_{BT} from NLRHA exceeded the design predictions from RSA. Part of the differences can be attributed to the damping level assumed in both analyses: NBC design spectrum based on 5% damping used in RSA compared to 3% damping assigned in NLRHA. The differences



on Δ_T are small and could be deemed acceptable for the C-T/C frames. For the other systems, the differences are due to system responses and should be addressed in design. Time history of storey drifts are presented in Fig. 5 under ground motions from a shallow crustal earthquake and an interface subduction earthquake. Hysteretic responses of the vertical bracing elements under the second ground motion record are given in Fig. 6. Under both records, the buildings with the C-T/C frames displayed stable response with peak drifts at diaphragm mid-span less than 1.4% h_n . This is essentially because of the limited inelastic deformations that took place in the CBFs as a result of their inherent overstrength (Fig. 6). Conversely, extensive yielding took place in the C-T/O and EBF SFRSs. Braces in the former sustained cumulated plastic elongation resulting in progressive drifting and permanent lateral deformations. The EBF system showed stable hysteretic behaviour but experienced large inelastic excursions resulting in significant storey drifts and link plastic rotations. This response may be due to the lower probable resistance and limited post-yielding stiffness of the system. Permanent residual deformations are less important, however, than those observed for the T-T/O system.

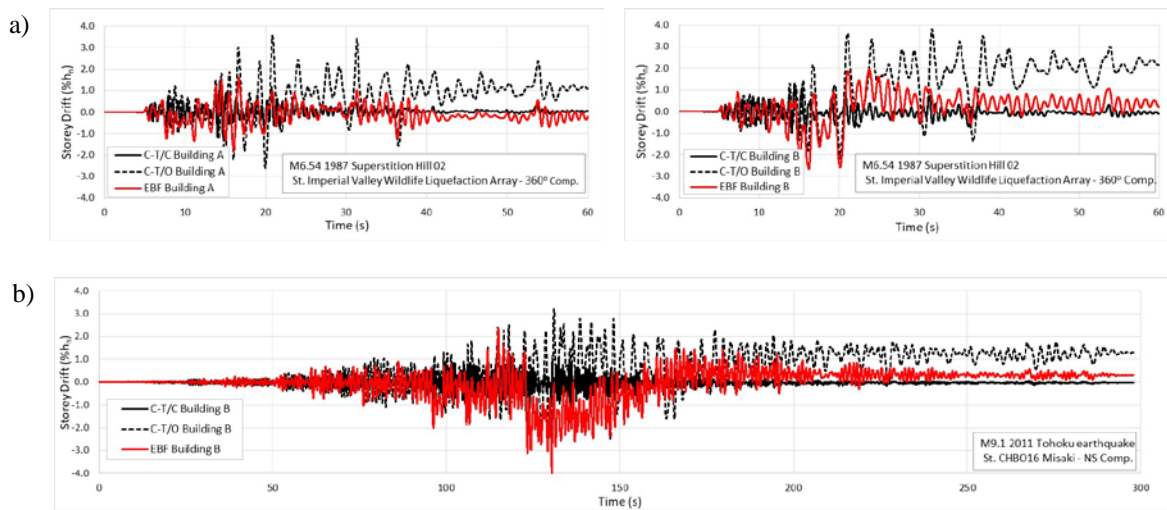


Fig. 5 – Storey drift responses at diaphragm mid-span of: a) Buildings A and B under a shallow crustal earthquake record; b) Building B under an interface subduction earthquake record

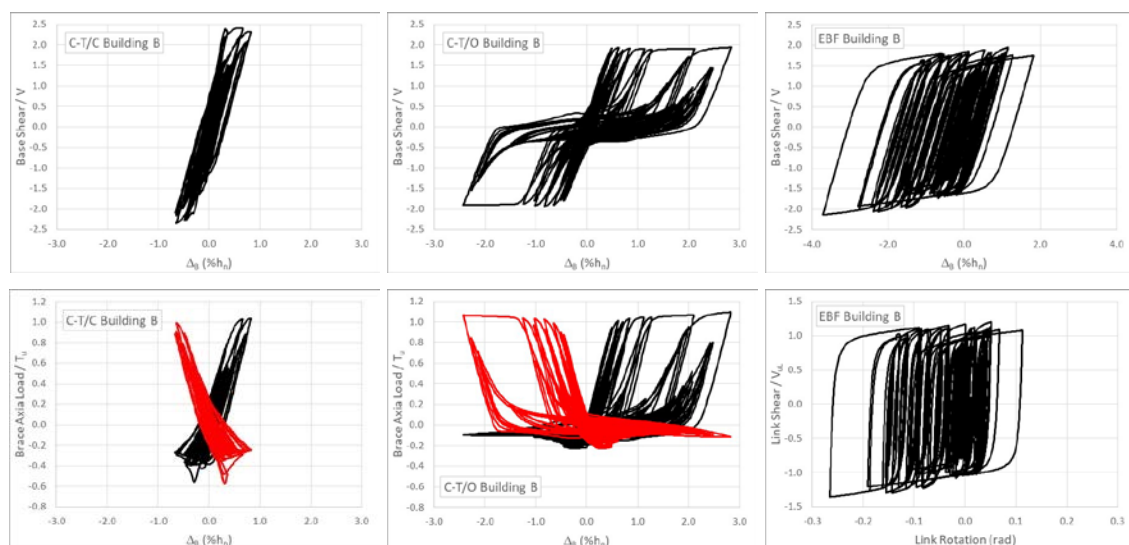


Fig. 6 – Storey shear-storey drift response (1st row) and force-storey drift response of the SFRS yielding elements (2nd row) for Building B under an interface subduction earthquake record (see Fig. 5b)



Time history responses of diaphragm shears at the diaphragm end and quarter span are plotted in Fig. 7a for the three SFRSs used for Building B. As anticipated from RSA, shears at $x/L = 0$ is dominated by first mode response whereas shears at $0.25 L$ are greatly influenced by mode 3 response, especially for the C-T/O and EBF systems when they experience large inelastic excursions during which lateral stiffness governing first mode response is reduced. Envelopes of the peak diaphragm shears along the diaphragm span are plotted for the same structures in Fig. 7b. The results indicate that the shear demand can be well predicted with the proposed modified RSA method for the C-T/C frames experiencing low ductility. These predictions however underestimate diaphragm shear forces for the other two systems.

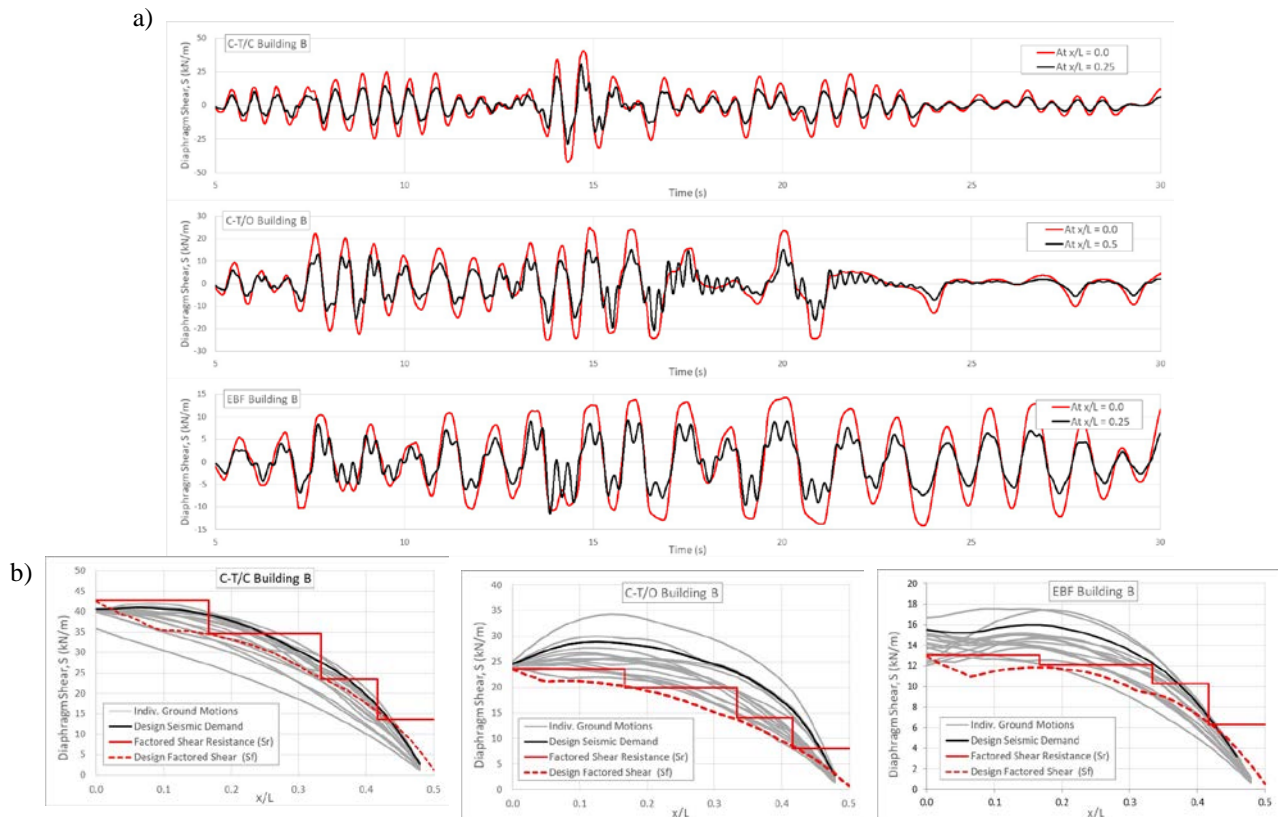


Fig. 3 – Diaphragm shears in Building B: a) Time history of diaphragm shears at $x/L = 0.0$ and 0.25 under the shallow crustal earthquake of Fig. 5a; b) Envelope of peak diaphragm shears over diaphragm half-span

3.3 Building 2xB with an interior bracing line

The roof diaphragm design and the vertical bracing of Building B were used for each portion of the 2xB Building. A new design was performed only for the interior braced frames using twice the seismic loads considered for the braced frames of Building B. This approach would typically be adopted in practice assuming that the individual rectangular portions of the building would behave as if they were not connected because of the diaphragm continuity at the connection is weakened by diaphragm shear flexibility. Properties of the interior braced frames are given in Table 1. Because of their larger brace sizes, these frames possessed slightly lower probable resistances compared to the frames along the end walls ($V_u/V = 2.41$ vs 2.54). The lateral stiffness of the interior frames was also equal to only 87% of twice the stiffness of the end braced frames. NLRHA showed that the structure behaved like a 182.4 m long building with inelastic deformations concentrating in the interior braced frames, as revealed by the Δ_{BT} values reported in Table 3. These results suggest that special design provisions are needed to avoid concentration of the inelastic demand in vertical bracing elements of single-storey buildings with flexible roof diaphragms and interior bracing.



4. Conclusions

The seismic provisions for single-storey steel buildings with flexible roof diaphragms of the NBC 2015 were described and methods were suggested to evaluate the roof diaphragm shear and bending moments and the deformation demands on the vertical bracing elements. These provisions and proposed methods were applied for two prototype buildings built with T/C CBFs, T/O CBFs and EBFs. The seismic response of the structures was then examined through NLRHA. Using EBFs or T/O CBFs can reduce considerably diaphragm design forces compared to the more common T/C CBFs. The methods proposed for predicting diaphragm forces and deformations in the braced frames gave satisfactory results for the buildings with T/C CBFs but significantly underestimated the demands for the EBFs and T/O CBFs. Further research is needed to improve design predictions and achieve adequate response for these two systems. A design methodology is also needed to ensure uniform inelastic demand in braced frames of structures with interior bracing lines.

5. References

- [1] Tremblay R, Stiemer SF (1996): Seismic Behavior of Single-Storey Steel Structures with Flexible Diaphragm. *Can. J. of Civ. Eng.*, **23** (1), 49-62.
- [2] Medhekar MS, Kennedy DJL (1999): Seismic Evaluation of Single-Storey Steel Buildings. *Can. J. of Civ. Eng.*, **26** (4), 379-394.
- [3] Tremblay R, Rogers A (2005): Impact of Capacity Design Provisions and Period Limitations on the Seismic Design of Low-Rise Steel Buildings. *Int. J. of Steel Structures*, **5**(1), 1-22.
- [4] Paultre P, Proulx J, Ventura CE, Tremblay R, Rogers C, Lamarche CP, Turek M (2004): Experimental Investigation and Dynamic Simulations of Low-Rise Steel Buildings for Efficient Seismic Design. *Proc. 13th World Conf. on Earthquake Eng.*, Vancouver, Canada, Paper no. 2919.
- [5] Lamarche CA, Proulx J, Paultre P, Turek M, Ventura CE, Le TP, Lévesque C (2009): Toward a better understanding of the dynamic characteristics of single-storey braced steel frame buildings in Canada. *Can. J. of Civ. Eng.*, **36**(6): 969-979.
- [6] Trudel-Languedoc S (2014): *Analyse du comportement sismique des bâtiments de faible hauteur en acier avec diaphragmes flexibles au toit*. M.Sc. Thesis, CGM Dept., Polytechnique Montreal, Montreal, QC (in French)
- [7] Trudel-Languedoc S, Tremblay R, Rogers CA (2014): Dynamic seismic response and design of single-storey structures with flexible steel roof deck diaphragms. *Proc. 10th National Earthquake Eng. Conf.*, Anchorage, AK, Paper No. 387.
- [8] Mortazavi P, Humar J (2015): Magnification of Internal Forces in the Flexible Diaphragm of a Single-Storey Buildings. *Proc. 11th Can. Conf. on Earthquake Eng.*, Victoria, BC, Paper No. 94155.
- [9] Tremblay R, Rogers CA (2017): Canadian provisions for the seismic design of single-storey steel buildings with flexible roof diaphragms. *Proc. 16th World Conf. on Earthquake Eng.*, Santiago, Chile, Paper No. 2837.
- [10] Humar J, Popovski M (2013): Seismic response of single-storey buildings with flexible diaphragms. *Can. J. of Civ. Eng.*, **40**, 875-886.
- [11] NRCC (2015): *National Building Code of Canada 2015*, 14th ed., National Research Council of Canada, Ottawa, ON.
- [12] ASCE (2017): *ASCE/SEI 41-17, Seismic Evaluation and Retrofit of Existing Buildings*. American Society of Civil Engineers (ASCE), Reston, VI.
- [13] CSA (2014): *CSA-S16-14, Design of steel structures*. Canadian Standards Association, Mississauga, ON.
- [14] AISI (2016): *AISI S310-16, North American Standard for the Design of Profiled Steel Diaphragm Panels*. American Iron and Steel Institute (AISI), Washington, DC.
- [15] NRCC (2017): *Structural Commentaries (User's Guide – NBC 2015: Part 4 of Division B)*, 4th ed. National Research Council of Canada, Ottawa, ON.
- [16] Aguerro A, Izvernari C, Tremblay R (2006): Modelling of the Seismic Response of Concentrically Braced Steel Frames using the OpenSees Analysis Environment. *Int. J. of Advanced Steel Construction*, **2**(3), 242-274.
- [17] Koboevic S, Rozon J, Tremblay R (2012): Seismic performance of low-to-moderate height eccentrically braced steel frames designed for North American seismic conditions. *J. Struct. Eng.*, **138**(12), 1465-1476.